Engineering Geology 204 (2016) 23–32

Contents lists available at ScienceDirect

Engineering Geology

journal homepage: www.elsevier.com/locate/enggeo

Laboratory investigation of liquefaction mitigation in silty sand using nanoparticles

Yu Huang [a,b,*], Lin Wang [a]

[a] Department of Geotechnical Engineering, College of Civil Engineering, Tongji University, Shanghai 200092, China
[b] Key Laboratory of Geotechnical and Underground Engineering, Ministry of Education, Tongji University, Shanghai 200092, China

ARTICLE INFO

Article history:
Received 13 June 2015
Received in revised form 19 January 2016
Accepted 22 January 2016
Available online 25 January 2016

Keywords:
Liquefaction mitigation
Nanoparticle
Laponite
Silty sand
Dynamic triaxial tests

ABSTRACT

Nanomaterials are presented in this paper as a novel method of liquefaction mitigation that overcomes the limitations of traditional mitigation methods. The proposed method is different from traditional densification and chemical grouting methods: no ground disturbance occurs and an entire site can be treated. In this study, laponite, synthetic silicate nanoparticles that are nontoxic, pure, highly plastic, and smaller in size than natural clay particles, has been selected as a representative nanomaterial that can be used in conjunction with liquefiable silty sand. Little research has been undertaken on the mixing of such materials. The cyclic behavior and liquefaction resistance of mixtures of laponite and silty sand have been studied by means of dynamic triaxial tests. The pore pressure accumulation process and deformation properties are compared between pure silty sand and laponite–silty sand samples to verify the effect of laponite on the liquefaction mitigation of the silty sand. Additionally, the viscosity of laponite suspensions is measured to determine the appropriate gel time for curing the laponite–silty sand samples. Microstructural imaging with a scanning electron microscope is analyzed in conjunction with liquefaction mitigation mechanisms. Then the effects of laponite concentration and curing time on the liquefaction resistance of the treated samples are discussed. This work provides experimental data to support the beneficial effects of laponite mixing on the reduction of liquefaction susceptibility in saturated silty sand. It also assesses the mechanisms and effects of nanoparticles on liquefaction potential.

1. Introduction

In recent years, large destructive earthquakes, such as the 2008 Wenchuan earthquake in China, the 2010 Chile earthquake, and the 2011 Great East Japan Earthquake, have resulted in multiple geo-engineering problems, of which liquefaction is particularly prominent (Juang and Li, 2007; Huang and Yu, 2013). Liquefaction is a phenomenon marked by a rapid and dramatic loss of soil strength; it occurs in loose, saturated soil deposits subjected to earthquake motion. The onset of liquefaction is usually sudden. The liquefiable soil's shear strength and shear modulus decrease significantly, resulting in the loss of soil bearing capacity, significant deformation, and soil settlement. This in turn leads to instability and destruction of structures such as building foundations, roads, bridges, and ports, sometimes causing serious losses of life and property (Huang and Jiang, 2010; Verdugo, 2012; Yasuda et al., 2012). Bird and Bommer (2004) examined fifty destructive earthquakes worldwide and found that liquefaction occurred in 62% of those earthquakes, causing 15%–30% of the earthquake damage. Therefore, research on liquefaction mitigation and control is of great importance.

Ground improvement techniques are commonly used to increase the liquefaction resistance of soils and control potential deformation. Traditional in situ liquefaction mitigation methods can be classed in two main categories: in situ densification and grouting. In situ densification methods include deep mixing (Porbaha et al., 1999), dynamic compaction (Shenthan et al., 2004; Yasrobi and Biglari, 2007), and granular piles (Krishna, 2011); these methods can effectively raise the bearing capacity and liquefaction resistance of the soil. However, they have limited applications because they can cause considerable disturbance to ecological and residential environments. Hence, in situ densification is more suitable for open undeveloped sites than for developed sites. Grouting can be used in constrained sites; traditional grouting materials include cement slurry, sodium silicate ($Na_2O \cdot nSiO_2$), and chemical grouts (such as acrylate and epoxy). Cement slurry has a high initial viscosity; therefore, cement grouts are usually injected under high pressure and often are used to form grout columns rather than to permeate the entire area beneath the structure. Chemical grouts present a high risk of damage to adjacent buildings and pollution of waterways if handled improperly (Vik et al., 2000). Therefore, with increased industrialization and urbanization and the progress of creative science

* Corresponding author at: Department of Geotechnical Engineering, College of Civil Engineering, Tongji University, Shanghai 200092, China.
E-mail address: yhuang@tongji.edu.cn (Y. Huang).

http://dx.doi.org/10.1016/j.enggeo.2016.01.015
0013-7952/

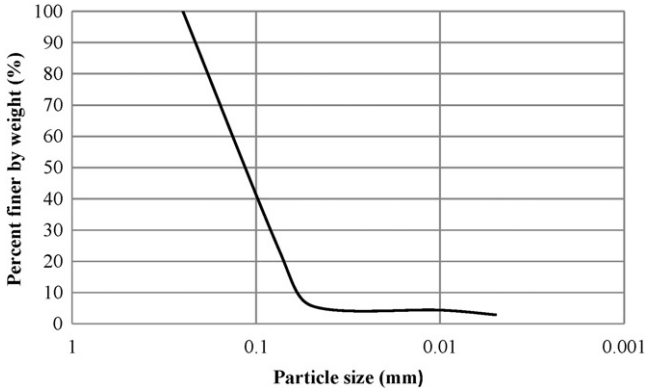

Fig. 1. Grain size distribution of silty sand.

and technology, alternative methods and materials for mitigating liquefaction risks should be explored (Huang and Wen, 2015).

Previous research on liquefaction mitigation has shown that fine plastic materials, such as clay-sized particles (<0.002 mm), can effectively enhance the liquefaction resistance of cohesionless soil (Dimitrova and Yanful, 2012; Ku and Juang, 2012; Kumar et al., 2013). Studies have found a threshold value for the content of clay particles. Below this value, the liquefaction resistance decreases with increasing clay particle content, but above this value, the rule is opposite (Gratchev et al., 2006, 2007; Abedi and Yasrobi, 2010). A chemically modified bentonite suspension has been proved to form a thixotropic gel and improve the liquefaction resistance by modifying the pore fluid between sand grains (El Mohtar et al., 2008). To lower the initial yield stress and viscosity of bentonite suspensions, and therefore help to improve the likelihood of grouting permeation, 0.5–2% sodium pyrophosphate can be added to the soil (Rugg et al., 2011; El Mohtar et al., 2013). Moreover, Witthoeft et al. (2012) proved the effectiveness of bentonite suspension in liquefaction mitigation at field scales using the finite difference method FLAC and thereby verified the scope of the soil reinforcement.

The U.S. National Research Council (2006) gives credit for the first steps in nanotechnology research to soil scientists and engineers whose studies focused on clay-sized particles. Colloidal silica (CS), an aqueous dispersion of silica nanoparticles sized 7–22 nm (Chang and Liu, 1994), was introduced into soil for site remediation (Persoff et al., 1994, 1999). In a recent liquefaction mitigation approach, the diluted CS was slowly injected from the edge of the injection site and transported through natural or artificial groundwater flow into the target position where it subsequently gelled and stabilized the liquefiable site (Gallagher, 2000; Gallagher and Mitchell, 2002). The feasibility and efficacy of CS grouting for the mitigation of liquefaction risk were then verified using centrifugal model tests (Gallagher et al., 2007a) and full-scale field tests (Gallagher et al., 2007b). Similar research findings on the liquefaction mitigation effects using CS have been presented by other researchers (Kodaka et al., 2005; Díaz-Rodríguez et al., 2008; Mollamahmutoglu and Yilmaz, 2010).

Recent studies indicate that synthetic nanoparticles of laponite show promise for use in sand liquefaction mitigation (El Mohtar, 2008). Laponite particles are smaller than clay particles and almost a tenth the size of bentonite particles; therefore, theoretically laponite has advantages for penetrating into finer soils. As laponite has good rheological properties and forms a transparent suspension once dispersed in water, it is usually chosen as a representative material in colloidal science (Levitz et al., 2000; Tanaka et al., 2004; Paula et al., 2009). Preliminary research on the use of laponite for mitigating liquefaction potential has focused on the microstructural characteristics of laponite particles and the rheological properties of laponite suspensions. The results show that laponite has better material properties and conductivity than bentonite (Howayek, 2011; Howayek et al., 2014). So far, however, no experimental data have been published on the cyclic characteristics and liquefaction resistance of liquefiable soil treated with laponite. Moreover, the liquefiable sands used in previous tests were usually pure sands, even though liquefaction of silty sand is not uncommon in seismic events. For example, extensive liquefaction phenomena of silty sands were observed in the Emilia-Romagna region after the 2012 Northern Italy earthquake sequence (Lombardi and Bhattacharya, 2014) and in Southern Taiwan after the 2010 Jiasian earthquake (Chang et al., 2011).

This paper presents the results of a laboratory investigation into liquefaction mitigation of silty sand mixed with laponite in a series of dynamic triaxial tests. The liquefaction resistance and cyclic behavior of laponite–silty sand samples were evaluated, providing experimental data to support the efficacy of laponite for liquefaction mitigation in

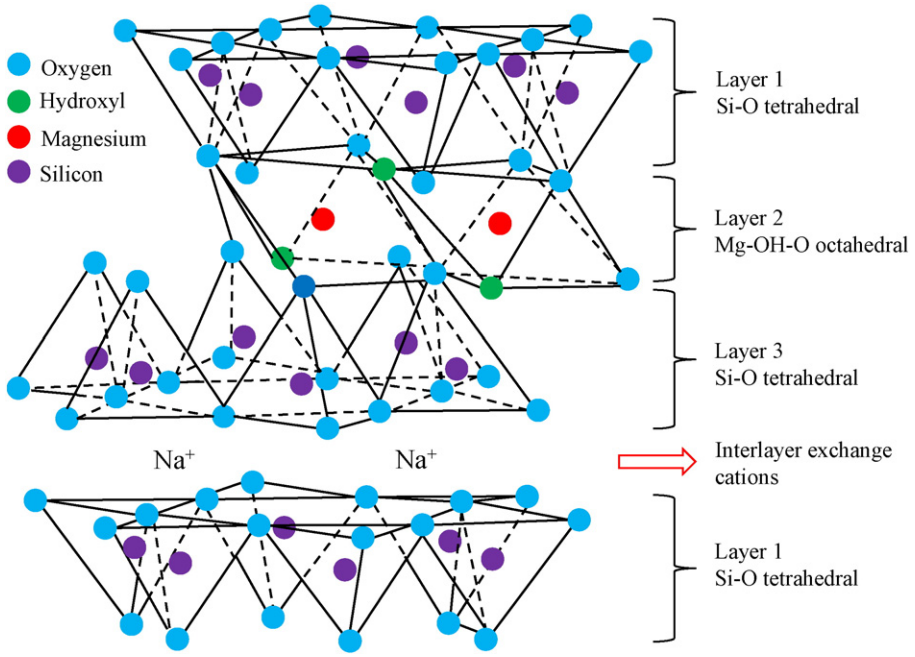

Fig. 2. Idealized structural formula of laponite (based on Rockwood Additives Ltd., 2011).

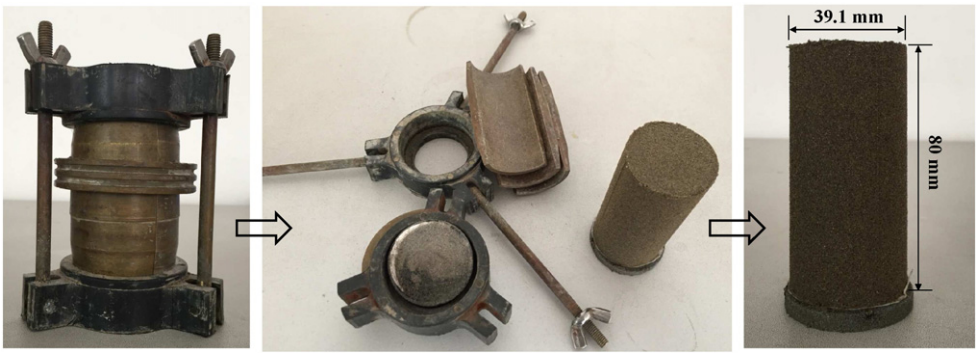

Fig. 3. Sample compaction container and a typical cylindrical laponite–silty sand specimen.

silty soil deposits. In addition, the rheological properties of laponite suspension were measured by rheology tests, and the microstructure of laponite–silty sand mixtures was investigated with scanning electron microscope (SEM) study. The experimental results reveal the liquefaction mitigation mechanism. Furthermore, two important factors, the laponite content and curing time, and their effects on the liquefaction resistance of treated samples, are also discussed.

2. Experimental materials

2.1. Silty sand

Silt and silty sand with the potential for liquefaction is widely distributed throughout the Shanghai region (Huang et al., 2008). The silty sand used in this experimental investigation was natural soil taken from a reservoir embankment on Changxing Island, Shanghai. According to a series of laboratory soil tests, the physical and mechanical properties of the silty sand used in this study are as follows: natural water content w = 19.4%, specific gravity G_s = 2.69, and specific weight g = 17.0–18.1 kN/m^3. The grain size distribution of the silty sand is shown in Fig. 1.

2.2. Laponite

In this study, laponite was chosen to be the representative nanomaterial. It is a synthetic layered silicate nanoparticle with a thickness of 1 nm and a diameter of 25 nm (Kroon et al., 1998). Laponite is made from a synthetic sheet of silicate nanoparticles, with layered structures of two tetrahedral layers and one octahedral layer, similar to a natural montmorillonite structure (Fig. 2). Because some of the bivalent magnesium ions on the particle surface are replaced by a lithium ion valence, the particle surface emits a large number of negative charges. Hydroxides on the edge such as Mg-OH and S-OH take a small amount of positive charge for protonation. Its chemical composition is 65.82% SiO_2, 30.15% MgO, 3.20% Na_2O, and 0.83% Li_2O, corresponding to the general formula as follows: $Na^{+0.7}$ [Si_8 $Mg_{5.5}$ $Li_{0.3}$ H_4 O_{24}]$^{-0.7}$ (Paula et al., 2009; Howayek, 2011). The laponite used in this study was stored in a plastic bag inside a container that was kept in a dry room to avoid absorption of humidity from the atmosphere.

3. Experimental methods

3.1. Specimen preparation

We investigated the liquefaction resistance of clean silty sand and silty sand treated with laponite through dynamic triaxial tests. To prepare the laponite–silty sand specimens, we dry mixed the silty sand and laponite during specimen preparation rather than using grouting permeation because the grouting permeation method is very sensitive and difficult to control (Persoff et al., 1999). Therefore, the dry mixing method was chosen to maximize reproducibility. Although the field injection process was not simulated, the grout material and soil properties were accurately represented.

The laponite–silty sand specimen preparation method was modified from standard procedures (GB/T50123-1999) to accommodate the specific nature of the tested materials. The preparation method is described below: silty sand and laponite were dry mixed by shaking in an airtight container. Then deionized de-aired water was added to the dry laponite–sand matrix to represent the natural water content. The concentration of the laponite suspension was determined by the ratio of dry laponite particles to added deionized de-aired water. To evaluate the effects of laponite concentration on the liquefaction resistance of the laponite–silty sand mixtures, four different laponite concentrations: 2.0%, 2.5%, 3.0%, and 3.5%, were prepared. Then, the mixtures of laponite–silty sand and water were compacted in a sample compaction container composed of a three-way split former. The prepared cylindrical soil specimens were 39.1-mm long with a diameter of 80 mm. The sample compaction container and a typical cylindrical laponite–silty sand specimen are shown in Fig. 3. To evaluate the effects of curing time on the liquefaction resistance of the specimens, the curing time was established using rheological tests. Then, based on the results of the viscosity test of the laponite suspension, the mixture samples were cured in a constant-temperature room (23 °C) for the required gel time. Pure silty sand samples were prepared as comparison samples in the same manner, but without the addition of the dry laponite particles. All samples presented in this paper have the same skeletal relative density.

3.2. Test procedures

In this study, dynamic triaxial tests were performed on specimens of liquefiable pure silty sand and silty sand mixed with different concentrations of laponite, using the GDS dynamic triaxial apparatus and associated software. The apparatus has a unidirectional vibration system

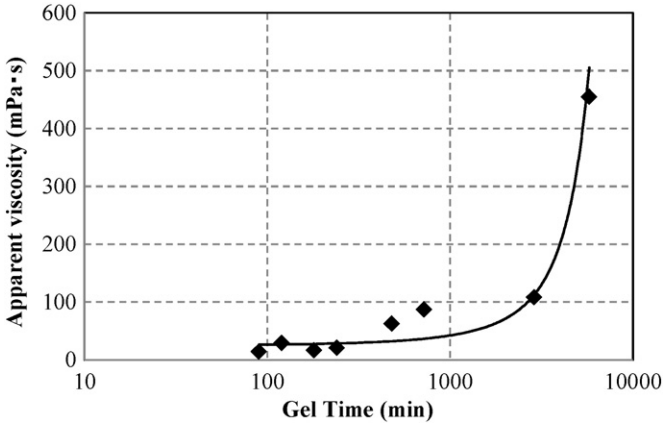

Fig. 4. Apparent viscosity versus gel time for 3% laponite suspension.

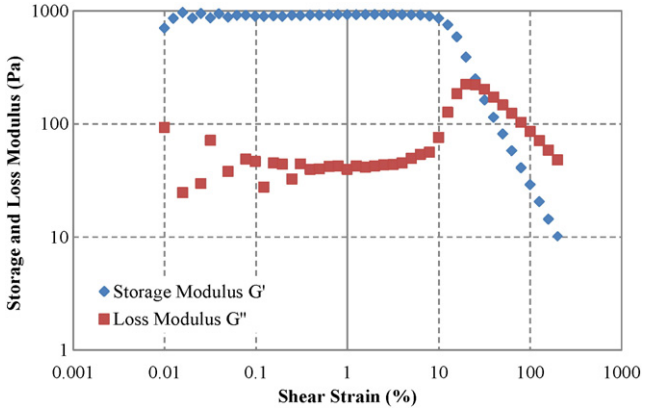

Fig. 5. Amplitude sweep test on 3% laponite suspension after 48 h.

and variable frequency, amplitude, and waveform that can be adjusted according to the test requirements. The specimens for the cyclic triaxial tests were back-pressure saturated, then isotropically consolidated to the desired effective confining stress, 30 kPa, to represent shallow soil field conditions. Undrained conditions were chosen to simulate dynamic earthquake loading in the field. All of the dynamic cyclic tests were performed using a sinusoidal waveform applied at a frequency of 0.1 Hz with stress reversal, starting with compression loading. It should be mentioned that a frequency of 0.1 Hz was applied to ensure the smooth operation of the GDS apparatus. In an early pre-experimental stage, we observed that when the forcing frequency was increased, e.g., to 1 Hz, the confining pressure produced too much fluctuation, leading to intense vibration of the apparatus. In addition, previous research (Hyodo et al., 1998; Xenaki and Athanasopoulos, 2003; Lombardi et al., 2014) showed that frequency does not appreciably affect the experimental results and the value of 0.1 Hz was chosen for

Table 1
Results of dynamic triaxial tests on laponite–silty sand samples at different laponite concentrations (0%, 2.0%, 2.5%, 3.0%, and 3.5%) after different curing periods (2, 4 and 6 days).

Test no.	Content of laponite suspension (%)	Curing time (days)	Initial effective cell pressure (kPa)	Cyclic stress (kPa)	Cyclic stress ratio, CSR	Cycles to liquefaction
1	0	2	30	7.2	0.12	124
2				8.4	0.14	31
3				10.8	0.18	3
4	2.0	2	30	9.6	0.16	55
5				10.8	0.18	25
6				12.0	0.20	17
7				13.2	0.22	5
8	2.0	4	30	10.8	0.18	79
9				12.0	0.20	18
10				13.2	0.22	9
11	2.0	6	30	12.0	0.20	48
12				13.2	0.22	20
13				15.0	0.25	5
14	2.5	2	30	12.0	0.20	30
15				13.2	0.22	15
16				13.8	0.23	8
17				15.0	0.25	7
18	3.0	2	30	12.0	0.20	44
19				13.8	0.23	15
20				15.6	0.26	8
21				18.0	0.30	4
22	3.0	4	30	12.0	0.20	65
23				13.8	0.23	16
24				16.8	0.28	8
25	3.0	6	30	12.0	0.20	83
26				15.0	0.25	7
27				18.0	0.3	20
28	3.5	2	30	13.8	0.23	22
29				15.0	0.25	19
30				18.0	0.30	10
31				19.2	0.32	5

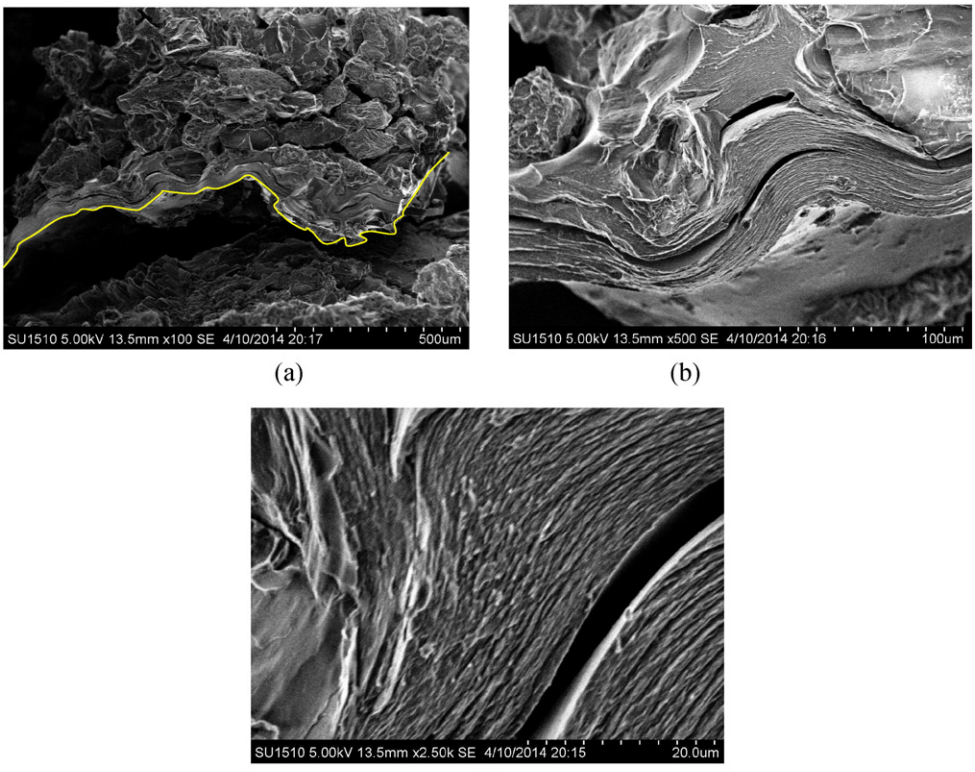

Fig. 6. Microstructure of 3% laponite–silty sand sample under various magnifications: (a) ×100, (b) ×500, and (c) ×2500.

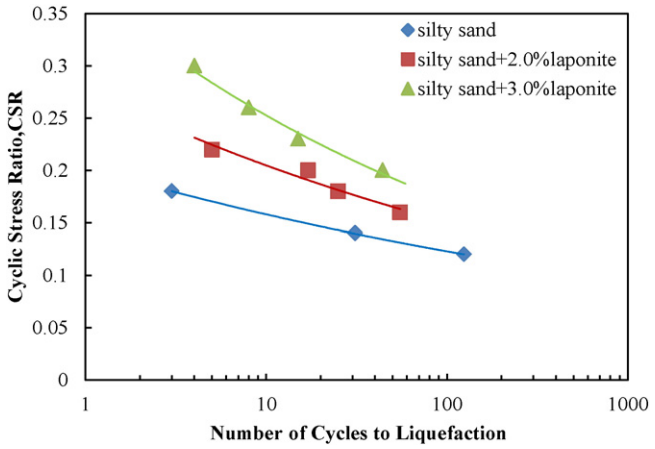

Fig. 7. CSR versus number of cycles to liquefaction for laponite–silty sand samples at laponite concentrations of 0%, 2.0%, and 3.0%.

the liquefaction tests. Under continuous cyclic loading conditions, the pore pressure at the base of the soil specimen was monitored. Different criteria have been used in the literature to identify the number of cycles leading to liquefaction. In this work, the criterion used to determine the onset of liquefaction is 'initial liquefaction' (Seed and Lee, 1966), which occurs when the pore pressure exceeds the confining pressure. The potential for soil to liquefy is based on the cyclic stress ratio (CSR) that measures the shear demand on the soil induced by earthquakes, and the cyclic resistance ratio (CRR) that measures the shear strength of the soil. To evaluate the effectiveness of enhancing the liquefaction resistance, the relationships between CSR and number of cycles to liquefaction are obtained and compared in Section 4.3. The CRR values defined as the CSR causing liquefaction in a specified number of loading cycles (Idriss and Boulanger, 2008) are used to evaluate the relationships between the liquefaction resistance and laponite concentration, as well as curing time in Sections 5.1 and 5.2 respectively.

To obtain the mechanical properties of the laponite suspension, rheological tests were conducted using an ARES rheometer, which has plate-plate measuring systems. The viscosity growth rule of the laponite suspension measured by rheological tests contributes to the determination of the curing time of the laponite–silty sand specimen in the dynamic triaxial tests. The viscosity of the laponite suspension was measured and determined by a constant rate ramp test under a controlled shear rate condition. The viscosity value ($\eta_{1000/s}$) was selected to represent the viscosity that may be mobilized in the suspension during the injection process (Howayek, 2011). The viscoelastic properties of the laponite suspension were then measured with shear strain increasing; this test can obtain the storage modulus and the loss modulus by an amplitude sweep test.

To obtain direct insight into the microstructure of laponite–silty sand mixtures, the scanning electron microscope (SEM) investigation was undertaken using a Hitachi SU1500 SEM. The sample to be observed was a 3% laponite–silty sand mixture prepared in the same way as the samples used in the dynamic triaxial tests. Because the SEM samples should be dry, very rapid freezing by liquid nitrogen was used to solidify the specimen pore water instantaneously without destroying the microstructure.

4. The mechanism of liquefaction mitigation

4.1. Viscosity and modulus of laponite suspension

Fig. 4 shows the viscosity increase in the 3% laponite suspension sample with time. When laponite is added to water, it initially forms a low-viscosity suspension. After a period of time (called the gel time) it transforms into a high-viscosity gel. In this study, the viscosity of the laponite suspension remained low (no more than 20 mPa·s) during the 4 h immediately following the dispersal of the laponite power in the water. This characteristic of laponite suspension allows sufficient time for grouting or sample preparation. In the next few hours, the viscosity steadily increased. After 48 h, it rose rapidly within a short period, reaching a high viscosity (close to 500 mPa·s). This indicates that the laponite–silty sand mixture specimens need to cure for more than 2 days.

Amplitude sweep tests were performed to gain insight into the mechanical properties of the laponite suspension inside the mixture specimens under shear stress. As the shear strain increased at a constant frequency, the shear stress was measured. The shear stress can be expressed as the sum of the elastic component, represented by the storage modulus (G′), and the viscous component, represented by the loss modulus (G″) (Barnes et al., 1989). Fig. 5 shows the results of an amplitude sweep test conducted on a 3% laponite suspension after 48 h of curing. For shear strains up to 10% (the linear viscoelastic region), the storage modulus G′ remains basically constant and $G' \gg G''$. Once the shear strain exceeds a critical value (approximately 10% for the test shown), the storage modulus drops significantly and the laponite suspension becomes increasingly viscous.

These results demonstrate the sol–gel transition for the laponite suspension used in liquefaction. This rheological property of the laponite–silty sand mixture is not found in the stiff cement grout columns. When the laponite suspension transforms into gel, it acquires elastic properties that improve the resistance of the silty sand treated with

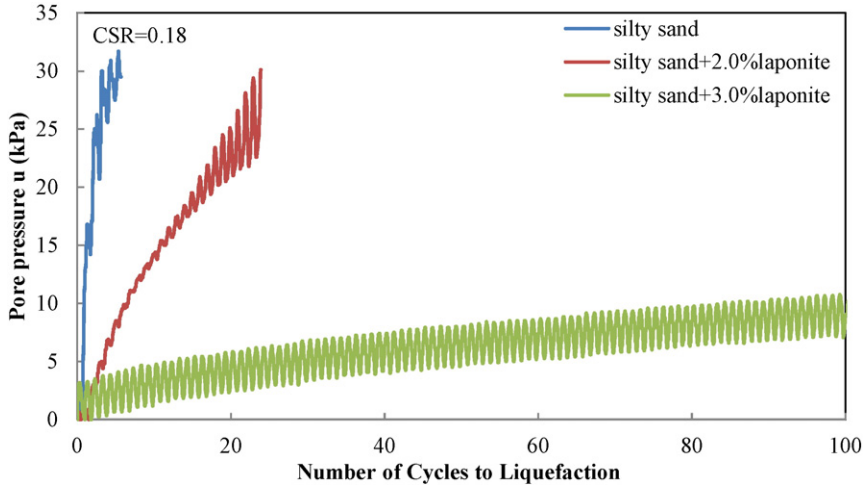

Fig. 8. Time series data for pore pressure of laponite–silty sand samples with laponite concentrations of 0%, 2.0%, and 3.0% at CSR = 0.18.

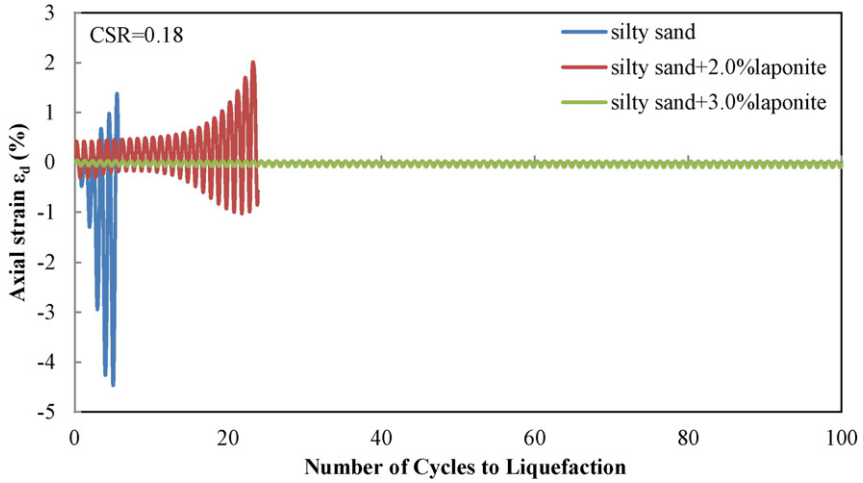

Fig. 9. Time series data for axial strain of laponite–silty sand samples with laponite concentrations of 0%, 2.0%, and 3.0% at CSR = 0.18.

laponite. However, the gel also loses its linearity and presents "thinning behavior" when the shear strain increases. Therefore, in the dynamic cyclic tests the pore pressure can be measured, which was not the case in previous research by Gallagher and Mitchell (2002). The behavior of the laponite–silty sand samples under cyclic loading is discussed later.

4.2. Microstructures of the silty sand–laponite mixture

Fig. 6 shows SEM micrographs of a 3% laponite–silty sand sample at different magnification factors: (a) ×100, (b) ×500, and (c) ×2500. In Fig. 6(a), the long marked structure is the laponite gel microstructure. The individual soil grains are cemented by laponite gel. Because silty sand contains clay particles, some flocculent structures can be observed on the grain surface. At higher magnification, the micrographs indicate that the laponite suspension prepared with deionized water has a plate-like microstructure with a regular pattern. This gel-like structure of the laponite gel suppresses the volumetric straining during cyclic loading and helps improve soil liquefaction resistance.

It is worth noting that in Fig. 6(a) the laponite gel does not completely fill the pores between the soil grains, leaving some space between the grains. This may occur because when the dry laponite particles are mixed with silty sand before the water is added, some laponite particles may be trapped at the sand contacts rather than being uniformly distributed inside the voids between the soil grains. Hence, when the saturated mixture samples are subjected to the dynamic cyclic tests, the free water in the residual space contributes to the measured pore pressure. The preparation of the laponite–silty sand specimen will thus influence the microstructure of the mixtures, as was shown in similar investigations on bentonite behavior (El Mohtar et al., 2013).

4.3. Liquefaction resistance and cyclic response

Based on the rheological test results, three different curing periods: 2, 4, and 6 days were chosen for the laponite–silty sand samples in the dynamic triaxial tests. The number of cycles to liquefaction was defined as the number of cycles required for the onset of liquefaction. The results of the dynamic triaxial tests on the laponite–silty sand samples at different laponite concentrations (0%, 2.0%, 2.5%, 3.0%, and 3.5%) after different curing periods (2, 4, and 6 days) are shown in Table 1. All of the samples were prepared with the same skeletal void ratio and isotropically consolidated under the same effective confining stress of 30 kPa. The liquefaction resistance comparison, pore pressure development, and axial strain development of the untreated and treated samples are analyzed first. The effects of the laponite concentration and curing time on the liquefaction resistance and pore pressure development of the treated samples are discussed next.

The effectiveness of the laponite suspension treatment was evaluated by comparing the cyclic resistance of the treated and untreated

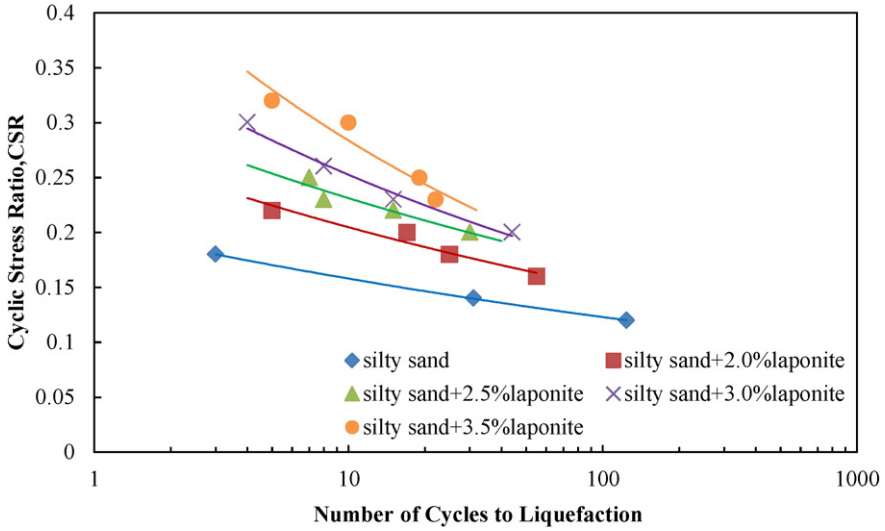

Fig. 10. CSR versus number of cycles to liquefaction for laponite–silty sand samples at laponite concentrations of 0%, 2.0%, 2.5%, 3.0%, and 3.5%.

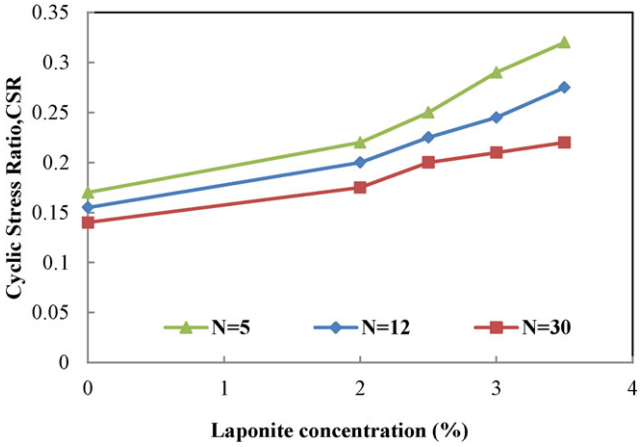

Fig. 11. CSR versus laponite concentration at different cycles (N = 5, 12, 30).

samples. Fig. 7 shows the liquefaction resistance of the pure silty sand sample and the 2.0% and 3.0% laponite–silty sand samples. The liquefaction resistance of the laponite–silty sand sample was considerably higher than that of the pure silty sand sample.

A sand specimen with added laponite can withstand more loading cycles for a given cyclic stress ratio (CSR) under undrained cyclic triaxial conditions before reaching liquefaction compared with a non-laponite treated specimen. In general, under equal CSR conditions, the untreated sand samples entered the liquid phase after fewer cycles compared with the treated samples. Once liquefaction occurred, the axial strain was larger, and with the increasing strain, sand sample destruction occurred. For the treated sand samples, the strain increase was small with increased duration of the vibration cycles and the sample remained intact. Figs. 8 and 9 show the time series data for the pore pressure and axial strain of the laponite–silty sand samples with different laponite concentrations (0%, 2.0%, and 3.0%) at CSR = 0.18.

As shown in Fig. 8, distinctly different pore pressure generation processes were observed between the treated and untreated samples. At the same CSR, the pore pressure of the pure silty sand sample increased rapidly to reach the confining pressure value (30 kPa) in three cycles of loading, resulting in the rapid loss of effective stress. However, for the 2% laponite–silty sand sample, the number of loading cycles to liquefaction increased to 24 cycles. The strongest effect of the laponite can be seen in the 3% laponite–silty sand sample: in 100 cycles of loading, the pore pressure increased to only 10 kPa — much lower than the confining pressure.

Fig. 9 shows that the axial strain expanding processes in the three samples are also significantly distinct. At the same CSR, the axial strain in the pure silty sand sample rose rapidly within about four cycles of loadings and the sample finally collapsed. The single amplitude axial strain of the untreated sample was almost 5%, more than twice that of the 2% laponite–silty sand sample, which was less than 2% when the pore pressure was equal to the confining pressure. No obvious axial strain was observed in the 3% laponite–silty sand sample and the sample remained intact over 100 loading cycles. The time series comparison shows that laponite can delay the pore water pressure generation process and restrict the strain expansion so that the liquefaction resistances of the treated samples are enhanced.

4.4. Liquefaction mitigation mechanism analysis

According to the results of the cyclic triaxial tests combined with rheological tests and SEM imaging, the liquefaction mitigation mechanism based on nanomaterials can be explained by the following processes. The most important process is fluid solidification in the soil pores between the grains. After the nanoparticles spread into the soil pore water, the nanoparticle suspension is transformed from a fluid to a gel similar to a soft solid gel because of the hydration process. Once the pore fluid is replaced by gel, a necessary condition for the triggering of liquefaction is eliminated because liquefaction always occurs in saturated fine soils. Moreover, unlike a fluid, the gel has shear resistance, which enhances the soil strength. The cementation of the soil grains by the gel also improves liquefaction resistance, with the viscosity of the gel increasing with time.

Conversely, because laponite gel has special thixotropy, its modulus will decrease as a result of the shearing action; the phase transformation from gel to liquid will be different from that of traditional cement grouting. Soil samples grouted by cement will retain their solid state once solidified; however, because of the laponite's thixotropy, in the dynamic triaxial tests of the laponite–silty sand samples, the pore pressure increased and liquefaction was still observed. Nevertheless, the onset of liquefaction was far slower than in the pure silty sand samples under the same loading conditions because the generation of pore pressure was delayed.

5. The effect of liquefaction mitigation

5.1. The effect of laponite content

To study the effect of laponite content on the liquefaction resistance of laponite–silty sand mixtures, we also conducted dynamic triaxial tests on 2.5% and 3.5% laponite–silty sand samples. The liquefaction resistances of the pure silty sand sample and 2.0%, 2.5%, 3.0%, and 3.5% laponite–silty sand samples are shown in Fig. 10. As the laponite concentration increases, the liquefaction resistance also increases. Note that the liquefaction resistance curves of the laponite–silt samples become steeper as the laponite content increases. This indicates that the resistance improvement due to laponite is stronger within the first few cycles than after many cycles. Thus, when the number of cycles increases, the soil resistance decreases because the laponite suspension undergoes “thinning behavior”.

For further comparison, the relationship between the cyclic stress ratios (CSR) representing liquefaction resistance and laponite concentration after a certain number of cycles is analyzed (Fig. 11). A magnitude 6.0 earthquake would be expected to generate five significant uniform stress cycles. Twelve cycles correspond to a magnitude 7.0 earthquake and thirty cycles correspond to a magnitude 8.0 earthquake. The CSRs of samples subjected to five cycles were 0.170, 0.220, 0.250, 0.285, and 0.320 for samples with laponite concentrations of 0%, 2.0%, 2.5%, 3.0%, and 3.5%, respectively. The increase in liquefaction resistance between samples with consecutively greater laponite concentrations was about 29.4%, 47.0%, 67.6%, and 88.2%. The same procedure can be easily adapted to obtain the CSRs of samples subjected to 12 or 30 cycles. The increase in liquefaction resistance can be seen in Table 2.

The results indicate that under the same curing time conditions, the effect of laponite content is more obvious for smaller magnitude earthquakes. In addition, 2% laponite by mass of suspension has been proven to mitigate liquefaction effectively. The small amount of nanomaterial required for effective liquefaction mitigation is a considerable

Table 2
Liquefaction resistance increase versus laponite concentration at different cycles (N = 5, 12, 30) for a curing time of 2 days.

Laponite concentration (wt.%)	N = 5		N = 12		N = 30	
	CSR	Liquefaction resistance increase (%)	CSR	Liquefaction resistance increase (%)	CSR	Liquefaction resistance increase (%)
0	0.170	/	0.155	/	0.140	/
2.0	0.220	29.4	0.200	29.0	0.175	25.0
2.5	0.250	47.0	0.225	45.2	0.200	42.8
3.0	0.285	67.6	0.245	58.1	0.210	50.0
3.5	0.320	88.2	0.275	77.4	0.220	57.1

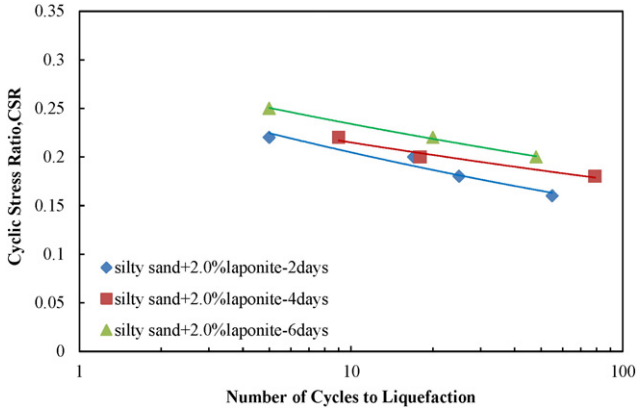

Fig. 12. CSR versus number of cycles to liquefaction for 2.0% laponite–silty sand samples after curing periods of 2, 4, and 6 days.

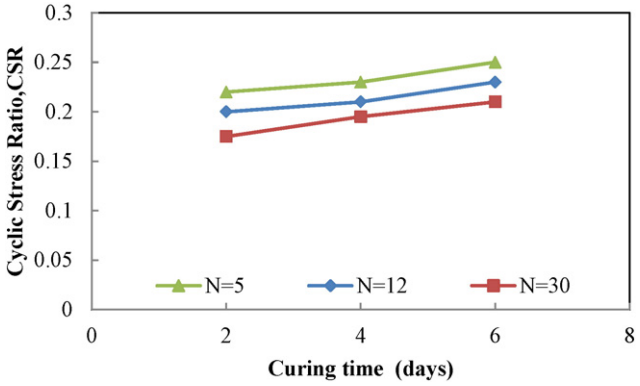

Fig. 14. CSR versus curing time for 2.0% laponite concentration at different cycles (N = 5, 12, 30).

advantage over other materials for liquefaction mitigation such as clay particles, bentonite, and colloidal silica.

5.2. The effect of curing time

As well as the effect of the laponite concentration on the liquefaction resistance of laponite–silty sand samples, the curing time is also an important factor affecting liquefaction resistance. For this reason, 2.0% laponite–silty sand samples and 3.0% laponite–silty sand samples were prepared with different curing times (2, 4, and 6 days) (Figs. 12 and 13, respectively). As expected, the liquefaction resistance of the laponite–silty sand mixtures improves as the curing time increases. The viscosity test results for the 3% laponite suspension show that the viscosity of the laponite suspension increases with time because of the thixotropy of the gel. It is this high viscosity that helps increase the soil's liquefaction resistance to cyclic loading as the soil particles contact and cementation increases.

In a similar way, the relationship between the cyclic stress ratios (CSR) representing the liquefaction resistance and the curing time at 5, 12, and 30 cycles were analyzed for laponite concentrations of 2% and 3% and shown in Figs. 14 and 15, respectively. The trend shows that the liquefaction resistance curve of the laponite–silt sample becomes slightly smoother as the curing time increases, indicating that prolonged curing after certain cycles will lead to a more significant improvement in liquefaction resistance than within the first few cycles. A comparison of the liquefaction resistance values for various curing times and cycle numbers can be seen in Tables 3 and 4 for laponite concentrations of 2% and 3%, respectively. The influence of the curing time is opposite to that of the laponite content, indicating that for the same laponite concentrations, the curing time would be more effective in larger magnitude earthquakes.

5.3. Other effect factors

According to above laboratory experiments, the effects of laponite concentration and curing time on the liquefaction resistance of the treated samples are discussed. In addition, several other factors may impact this treatment effectiveness, especially in large-scale engineering practice. The way of adding laponite to silty soil directly affects the homogeneity of the mixtures. If nanoparticles and liquable sand are not pretreated by desiccation and disintegration, they cannot be homogeneously mixed. For this reason, it's worth considering that nanoparticles can be injected into soil in the form of suspension. Suspension modification to decrease the initial viscosity and increase the likelihood of grouting permeation may help homogeneous distribution. For example, sodium pyrophosphate can be a feasible additive (Rugg et al., 2011; El Mohtar et al., 2013). Moreover, the new way in which CS suspensions are penetrated and controlled through radial injection wells and a central extraction well (Gallagher et al., 2007a; Conlee et al., 2012; Hamderi and Gallagher, 2015) can also be adopted to increase homogeneity. Hence, the large-scale effectiveness of stabilizing silty sand by using laponite needs to be investigated in next ensuing work.

Furthermore, the chemical compositions and properties of the porewater are not negligible effect factors. For example, previous rheological experimental research on laponite suspension has shown that pH and the concentration of added salt (Cs) affect the chemical stability and rheological behavior of laponite suspensions. Generally, laponite has a pH of 9.8 when it is dispersed in deionized water (Rockwood

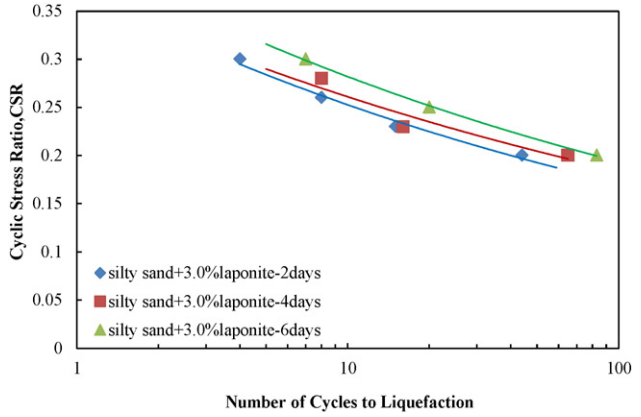

Fig. 13. CSR versus number of cycles to liquefaction for 3.0% laponite–silty sand samples after curing periods of 2, 4, and 6 days.

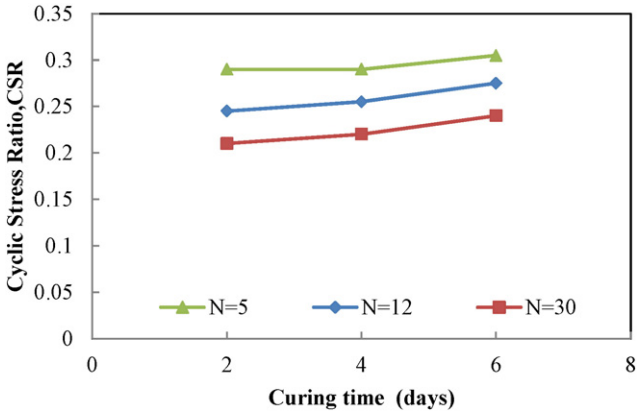

Fig. 15. CSR versus curing time for 3.0% laponite concentration at different cycles (N = 5, 12, 30).

Table 3
Liquefaction resistance increase versus curing time at different cycles (N = 5, 12, 30) for a laponite concentration of 2.0%.

Curing time (days)	N = 5		N = 12		N = 30	
	CSR	Liquefaction resistance increase (%)	CSR	Liquefaction resistance increase (%)	CSR	Liquefaction resistance increase (%)
2	0.220	/	0.200	/	0.175	/
4	0.230	4.5	0.210	5.0	0.195	11.4
6	0.250	13.6	0.230	15.0	0.210	20.0

Additives Ltd., 2011). However, it is reported that a decrease in pH (<9) will cause the dissolution of laponite because particles will become chemically unstable (Thompson and Butterworth, 1992; Cocard et al., 2000; Howayek, 2011). As for salinity, if the laponite suspension is at high Cs, it will have higher initial viscosity (Howayek, 2011); even separate into two domains due to the sedimentation of laponite aggregate (Mongondry et al., 2005). Therefore, a deeper research into the porewater chemical effects on the short-term and long-term properties of this treatment is needed.

6. Conclusions

Based on the novel concept of liquefaction mitigation with nanoparticles, some primary experimental studies including dynamic triaxial tests, rheology tests, and SEM imaging have been conducted. The feasibility and effectiveness of using laponite for liquefaction mitigation in silty sand was verified and its mechanisms analyzed. The main conclusions are as follows.

- The main mechanisms by which laponite mitigates liquefaction potential are pore fluid solidification, soil grain cementation, and the delay of pore pressure generation.
- The rheological properties of a sol–gel transition in a laponite suspension improves the liquefaction resistance, while at the same time its "thinning behavior" reduces the liquefaction resistance at higher cyclic loading.
- Laponite gel has a regular plate-like microstructure that cements individual soil grains. However, dry-mixing the laponite and silty sand during sample preparation leads to residual cavities beyond those formed by laponite gel and soil grains, and results in pore pressure measured in the dynamic cyclic tests.
- The liquefaction resistance of the laponite–silt samples is stronger than that of the pure silt samples. The pore pressure accumulation process in the treated samples is delayed and the deformation is much smaller compared with that of the untreated samples.
- As the laponite concentration or curing time increase in the laponite–silty sand samples, the liquefaction resistance improves accordingly. However, this trend deviates in two cases: (1) the effect of laponite concentration is stronger within the initial few cycles and (2) the effect of curing time is stronger after more cycles.

Table 4
Liquefaction resistance increase versus curing time at different cycles (N = 5, 12, 30) for a laponite concentration of 3.0%.

Curing time (days)	N = 5		N = 12		N = 30	
	CSR	Liquefaction resistance increase (%)	CSR	Liquefaction resistance increase (%)	CSR	Liquefaction resistance increase (%)
2	0.285	/	0.245	/	0.210	/
4	0.290	1.8	0.255	4.1	0.220	4.8
6	0.305	7.0	0.275	12.2	0.240	14.3

Acknowledgments

This work was supported by the National Natural Science Foundation of China (Grants Nos. 41372355 and 41511130069).

References

Abedi, M., Yasrobi, S.S., 2010. Effects of plastic fines on the instability of sand. Soil Dyn. Earthq. Eng. 30 (3), 61–67.
Barnes, H.A., Hutton, J.F., Walters, K., 1989. An Introduction to Rheology. Elsevier Science Publishers, Amsterdam, The Netherlands (199 pp.).
Bird, J.F., Bommer, J.J., 2004. Earthquake losses due to ground failure. Eng. Geol. 75 (2), 147–179.
Chang, S.Y., Liu, L., 1994. Preparation and properties of tailored morphology, monodisperse colloidal silica-cadmium sulfide nanocomposites. J. Am. Chem. Soc. 116 (15), 6739–6744.
Chang, W.J., Ni, S.H., Huang, A.B., Huang, Y.H., Yang, Y.Z., 2011. Geotechnical reconnaissance and liquefaction analyses of a liquefaction site with silty fine sand in Southern Taiwan. Eng. Geol. 123, 235–245.
Cocard, S., Tassin, J.F., Nicolai, T., 2000. Dynamical mechanical properties of gelling colloidal disks. Trans. Soc. Rheol. 585-594.
Conlee, C.T., Gallagher, P.M., Boulanger, R.W., Kamai, R., 2012. Centrifuge modeling for liquefaction mitigation using colloidal silica stabilizer. J. Geotech. Geoenviron. 138 (11), 1334–1345.
Díaz-Rodríguez, J.A., Antonio-Izarraras, V.M., Bandini, P., López-Molina, J.A., 2008. Cyclic strength of a natural liquefiable sand stabilized with colloidal silica grout. Can. Geotech. J. 45 (10), 1345–1355.
Dimitrova, R.S., Yanful, E.K., 2012. Factors affecting the shear strength of mine tailings/clay mixtures with varying clay content and clay mineralogy. Eng. Geol. 125, 11–25.
El Mohtar, C.S., 2008. Pore Fluid Engineering: An Auto Adaptive Design for Liquefaction Migration (Ph.D. Thesis) Purdue University, West Lafayette, Indiana, USA.
El Mohtar, C.S., Bobet, A., Santagata, M.C., Drnevich, V.P., Johnston, C.T., 2013. Liquefaction mitigation using bentonite suspensions. J. Geotech. Geoenviron. 139 (8), 1369–1380.
El Mohtar, C.S., Clarke, J., Bobet, A., Santagata, M., Drnevich, V., Johnston, C., 2008. Cyclic response of a sand with thixotropic pore fluid. Geotechnical Earthquake Engineering and Soil Dynamics IV, pp. 1–10.
Gallagher, P.M., 2000. Passive Site Remediation for Mitigation of Liquefaction Risk (Ph.D. Thesis) Virginia Polytechnic Institute and State University, Virginia, USA.
Gallagher, P.M., Mitchell, J.K., 2002. Influence of colloidal silica grout on liquefaction potential and cyclic undrained behavior of loose sand. Soil Dyn. Earthq. Eng. 22, 1017–1026.
Gallagher, P.M., Conlee, C.T., Rollins, K.M., 2007a. Full-scale field testing of colloidal silica grouting for mitigation of liquefaction risk. J. Geotech. Geoenviron. 133 (2), 186–196.
Gallagher, P.M., Pamuk, A., Abdoun, T., 2007b. Stabilization of liquefiable soils using colloidal silica grout. J. Mater. Civ. Eng. 19 (1), 33–40.
Gratchev, I.B., Sassa, K., Osipov, V.I., Fukuoka, H., Wang, G., 2007. Undrained cyclic behavior of bentonite–sand mixtures and factors affecting it. Geotech. Geol. Eng. 25, 349–367.
Gratchev, I.B., Sassa, K., Osipov, V.I., Sokolov, V.N., 2006. The liquefaction of clayey soils under cyclic loading. Eng. Geol. 86 (1), 70–84.
Hamderi, M., Gallagher, P.M., 2015. Pilot-scale modeling of colloidal silica delivery to liquefiable sands. Soils Found. 55 (1), 143–153.
Howayek, A.E., 2011. Characterization, Rheology and Microstructure of Laponite Suspensions (Master Thesis) Purdue University, West Lafayette, Indiana, USA.
Howayek, A.E., Bobet, A., Johnston, C.T., Santagat, M., Sinfield, J.V., 2014. Microstructure of sand–laponite–water systems using cryo-sem. Geo-Congress 2014 Technical Papers, ASCE, pp. 693–702.
Huang, Y., Jiang, X.M., 2010. Field-observed phenomena of seismic liquefaction and subsidence during the 2008 Wenchuan earthquake. Nat. Hazards 54 (3), 839–850.
Huang, Y., Wen, Z.Q., 2015. Recent developments of soil improvement methods for seismic liquefaction mitigation. Nat. Hazards 76 (3), 1927–1938.
Huang, Y., Yu, M., 2013. Review of soil liquefaction characteristics during major earthquakes of the twenty-first century. Nat. Hazards 65 (3), 2375–2384.
Huang, Y., Jin, C., Zhuang, Z.J., Zheng, Y.L., 2008. Experimental research on liquefaction characteristics of sandy silty sand layer ⑤$_2$ in Shanghai. J. Tongji Univ. (Nat. Sci.) 38 (1), 45–49 (in Chinese).
Hyodo, M., Hyde, A.F.L., Aramaki, N., 1998. Liquefaction of crushable soils. Géotechnique 48 (4), 527–543.
Idriss, I.M., Boulanger, R.W., 2008. Soil Liquefaction during Earthquakes. Earthquake Engineering Research Institute (EERI), Oakland, California, USA.
Juang, C.H., Li, D.K., 2007. Assessment of liquefaction hazards in Charleston quadrangle, South Carolina. Eng. Geol. 92, 59–72.
Kodaka, T., Ohno, Y., Takyu, T., 2005. Cyclic shear characteristics of treated sand with colloidal silica grout. Proceedings of the International Conference on Soil Mechanics and Geotechnical Engineering) 16(2). Aa Balkema Publishers, p. 401.
Krishna, A.M., 2011. Mitigation of liquefaction hazard using granular piles. Int. J. Geotech. Earthq. Eng. 2 (1), 44–66.
Kroon, M., Vos, W.L., Wegdam, G.H., 1998. Structure and formation of a gel of colloidal disks. Phys. Rev. E 57, 1962–1970.
Ku, C.S., Juang, C.H., 2012. Liquefaction and cyclic softening potential of soils — a unified piezocone penetration testing-based approach. Géotechnique 62 (5), 457–461.
Kumar, S.S., Krishna, A.M., Dey, A., 2013. Parameters influencing dynamic soil properties: a review treatise. Proceedings of the National Conference on Recent Advances in Civil Engineering, pp. 1–10.

Levitz, P., Lecolier, E., Mourhid, A., 2000. Liquid–solid transition of laponite suspensions at very low ionic strength: long-range electrostatic stabilization of anisotropic colloids. Europhys. Lett. 49 (5), 672–677.
Lombardi, D., Bhattacharya, S., 2014. Liquefaction of soil in the Emilia-Romagna region after the 2012 Northern Italy earthquake sequence. Nat. Hazards 73 (3), 1749–1770.
Lombardi, D., Bhattacharya, S., Hyodo, M., Kaneko, T., 2014. Undrained behaviour of two silica sands and practical implications for modelling SSI in liquefiable soils. Soil Dyn. Earthq. Eng. 66, 293–304.
Mollamahmutoglu, M., Yilmaz, Y., 2010. Pre- and post-cyclic loading strength of silica-grouted sand. Proc. ICE Geotech. Eng. 163, 343–348.
Mongondry, P., Tassin, J.F., Nicolai, T., 2005. Revised state diagram of laponite dispersions. J. Colloid Interface Sci. 283 (2), 397–405.
National Research Council, 2006. Geological and Geotechnical Engineering in the New Millennium: Opportunities for Research and Technological Innovation. National Academies Press, Washington, DC (222 pp.).
Paula, F.L.O., da Silva, G.J., Aquino, R., Depeyrot, J., Fossum, J.O., Knudsen, K.D., Helgesen, G., Tourinho, F.A., 2009. Gravitational and magnetic separation in self-assembled clay-ferrofluid nanocomposites. Braz. J. Phys. 39 (1), 163–170.
Persoff, P., Apps, J., Moridis, G., Whang, J.M., 1999. Effect of dilution and contaminants on sand grouted with colloidal silica. J. Geotech. Geoenviron. 125 (6), 461–469.
Persoff, P., Moridis, G.J., Apps, J., Pruess, K., Muller, S.J., 1994. Designing injectable colloidal silica barriers for waste isolation at the Hanford site. Proceedings of the 33rd Hanford Symposium on Health and the Environment: Symposium on In-situ Remediation—Scientific Basis for Current and Future Technologies, Richland, WA (United States). 1, pp. 87–101.
Porbaha, A., Zen, K., Kobayashi, M., 1999. Deep mixing technology for liquefaction mitigation. J. Infrastruct. Syst. 5, 21–34.
Rockwood Additives Ltd., 2011. Laponite Performance Additives. Spec. sheet.
Rugg, D.A., Yoon, J., Hwang, H., El Mohtar, C.S., 2011. Undrained shearing properties of sand permeated with a bentonite suspension for static liquefaction mitigation. Proceedings of the Geofrontiers, Dallas, TX, pp. 677–686.
Seed, H.B., Lee, K.L., 1966. Liquefaction of saturated sands during cyclic loading. J. Soil Mech. Found. Div. 92 (6), 105–134.
Shenthan, T., Nashed, R., Thevanayagam, S., Martin, G.R., 2004. Liquefaction mitigation in silty soils using composite stone columns and dynamic compaction. Earthq. Eng. Eng. Vib. 3 (1), 39–50.
Tanaka, H., Meunier, J., Bonn, D., 2004. Nonergodic states of charged colloidal suspensions: repulsive and attractive glasses and gels. Phys. Rev. E 69, 031404-1-6.
Thompson, D.W., Butterworth, J.T., 1992. The nature of laponite and its aqueous dispersions. J. Colloid Interface Sci. 151 (1), 236–243.
Verdugo, R., 2012. Comparing liquefaction phenomena observed during the 2010 Maule, Chile earthquake and 2011 great east Japan earthquake. Proceedings of the International Symposium on Engineering Lessons Learned from the 2011 Great East Japan Earthquake, Tokyo, Japan, pp. 707–718.
Vik, E.A., Sverdrup, L., Kelley, A., Storhaug, R., Beitnes, A., Boge, K., Grepstad, G.K., Tveiten, V., 2000. Experiences from environmental risk management of chemical grouting agents used during construction of the romeriksporten tunnel. Tunn. Undergr. Space Technol. 15 (4), 369–378.
Witthoeft, A.F., Santagata, M.C., Bobet, A., 2012. Numerical study of the effectiveness of bentonite treatment for liquefaction mitigation. Proc. GeoCongress 2012, 1958–1967.
Xenaki, V.C., Athanasopoulos, G.A., 2003. Liquefaction resistance of sand–silt mixtures: an experimental investigation of the effect of fines. Soil Dyn. Earthq. Eng. 23 (3), 1–12.
Yasrobi, S.S., Biglari, M., 2007. The use of dynamic compaction in liquefaction hazards mitigation at reclaimed lands in Assalouyeh petro-chemical complex—Iran. Soft Soil Eng. 587–593.
Yasuda, S., Harada, K., Ishikawa, K., Kanemaru, Y., 2012. Characteristics of liquefaction in Tokyo Bay area by the 2011 Great East Japan earthquake. Soils Found. 52 (5), 793–810.